Journal of Global Change Data & Discovery. 2024, 8(2): 132-146
www.geodoi.ac.cn

Global Change Research Data Publishing & Repository

Spatial Scenes-Based Ecological Carrying Capacity Dataset of the Guangdong-Hong Kong-Macao Greater Bay Area (1990–2019)

Wang, M. D.[1] Tang, Y. Z.[2] Shi, T. Z.[1*] Liu, Q.[3] Yan, F. Q.[4] Lv, P.[1]
Deng, D. P.[1], Zhang, Z. H.[1] Wang, Z. H.[4] Hu, Z. W.[1] Wu, G. F.[1]
Su, F. Z.[4]

1. MNR Key Laboratory for Geo-Environmental Monitoring of Great Bay Area & Guangdong–Hong Kong-Macau Joint Laboratory for Smart Cities & State Key Labora-tory of Subtropical Building and Urban Science, Shenzhen University, Shenzhen 518060, China;
2. Guangdong Laboratory of Artificial Intelligence and Digital Economy (SZ), Shenzhen 518107, China;
3. Department of Land Surveying and Geomatics, the Hong Kong Polytechnic University, Hong Kong 999077, China;
4. State Key Laboratory of Resources and Environmental Information System, Institute of Geographic Sciences and Natural Resources Research, Chines Academy of Sciences, Beijing 100101, China

Abstract: Taking Guangdong, Hong Kong and Macao Greater Bay Area as the study area, the authors completed the spatial scene classification data based on the object-oriented method; coupled with the three-dimensional ecological footprint method and established the spatial scene-based ecological carrying capacity dataset of the coastal zone (1990–2019). The overall accuracies of the spatial scene classification results for 1990, 2000, 2010 and 2019 were calculated using the confusion matrix to reach 85.10%, 82.72%, 80.19% and 80.65%, respectively. The content of this dataset includes the following data in the study area: (1) spatial distribution data of the spatial scenes of coastline, coastal zone and sea area in four historical periods (1990, 2000, 2010 and 2019); (2) data of land-sea variation of spatial scenes in every 10 years; and (3) data of ecological carrying capacity and ecological footprint change of coastal zone and sea area from 1990 to 2019. The dataset is archived in .shp, .tif and .xlsx formats, with a total of 58 files and a data size of 2.75 GB (compressed into 1 file, 8.97 MB).

Keywords: spatial scene; ecological carrying capacity; Guangdong-Hong Kong-Macao Greater Bay Area; coastal and maritime area

DOI: https://doi.org/10.3974/geodp.2024.02.03

Received: 15-03-2024; **Accepted:** 20-05-2024; **Published:** 25-06-2024

Foundations: National Natural Science Foundation of China (42306245, 41890854); Department of Science and Technology of Guangdong Province (2020B1212030009)

***Corresponding Author:** Shi, T. Z. GBX-5637-2022, MNR Key Laboratory for Geo-Environmental Monitoring of Great Bay Area of Shenzhen University, tiezhushi@szu.edu.cn

Data Citation: [1] Wang, M. D., Tang, Y. Z., Shi, T. Z., *et al*. Spatial scenes-based ecological carrying capacity dataset of the Guangdong-Hong Kong-Macao Greater Bay Area (1990–2019) [J]. *Journal of Global Change Data & Discovery*, 2024, 8(2): 132–146. https://doi.org/10.3974/geodp.2024.02.03. https://cstr.escience.org.cn/CSTR:20146.14.2024.02.03.

[2] Wang, M. D., Tang, Y. Z., Shi, T. Z., *et al*. Spatial scenes-based ecological carrying capacity dataset for the Guangdong-Hong Kong-Macao Greater Bay Area (1990–2019) [J/DB/OL]. *Digital Journal of Global Change Data Repository*, 2024. https://doi.org/10.3974/geodb.2024.06.03.V1. https://cstr.escience.org.cn/CSTR:20146.11.2024.06.03.V1.

CSTR: https://cstr.escience.org.cn/CSTR:20146.14.2024.02.03

Dataset Availability Statement:

The dataset supporting this paper was published and is accessible through the *Digital Journal of Global Change Data Repository* at: https://doi.org/10.3974/geodb.2024.06.03.V1 or https://cstr.escience.org.cn/CSTR:20146.11.2024.06.03.V1.

1 Introduction

The coastal zone and nearshore areas, situated at the interface of land and sea, constitute a complex "natural-social-economic" system[1]. These regions are characterized by a high density of land-sea interfaces and the people's interactions with them, and their sustainable development is directly related to human well-being and green circular economic development in the land and sea environments[2,3]. The coastal zone and nearshore areas of the Guangdong-Hong Kong-Macao Greater Bay Area (GBA) are characterized by a highly complicated geography, rich ecological systems, and a very developed social economy. Within the region, the Pearl River Delta is considered one of the world's largest and most compact deltas[4,5]. Over the past few decades, accompanying the steady economic development and population increase, the GBA's coastal area has faced escalating pressure on resources and the environment. This has led to a shift in the ecological security risk paradigm and its enhancement significantly[6]. Thus, the ecological carrying capacity of coastal and nearshore zones can be described as the capacity of these environments for the exploitation of resources and impacts of the environment under anthropogenic pressure[7]. Therefore, dynamic assessments of the ecological carrying capacity indicators will contribute to elaborate the scientific explanations of the drivers of the changes in sustainability in the region and, thus, will contribute to the further enhancement of sustainable regional development[8].

This dataset focuses on the coastal zone and marine areas of the Guangdong-Hong Kong-Macao Greater Bay Area. A spatial scene classification system and an ecological carrying capacity assessment framework for the GBA's coastal and marine areas have been established. Remote sensing data, socioeconomic data, and spatial planning documents were utilized as primary data sources. The study has generated two datasets: (1) a spatial-temporal distribution of spatial scenes, and (2) a dynamic evolution of ecological carrying capacity and ecological footprint for the study area from 1990 to 2019.

2 Metadata of the Dataset

The metadata of the spatial scenes-based ecological carrying capacity dataset of the Guangdong-Hong Kong-Macao Greater Bay Area (1990–2019)[9] is summarized in Table 1. The metadata includes the dataset's full name, short name, authors, year of dataset, temporal resolution, spatial resolution, data format, data size, data files, data publisher, and data sharing policy, etc.

3 Methods

The research area was established based on China's national coastal zone and tidal flat resource comprehensive survey regulations[11] and international exclusive economic zones[12]. A spatial scene classification system[14] for the study area was constructed, incorporating land cover, ecological function, dominant socio-economic attributes, and externalities, in conjunction with the "National Marine Functional Zoning"[13] by the State Oceanic Administration. Coastal land was categorized into forest, grassland, cropland, water bodies,

Table 1 Metadata summary of the spatial scenes-based ecological carrying capacity dataset of the Guangdong-Hong Kong-Macao Greater Bay Area (1990–2019)

Items	Description
Dataset full name	Spatial scenes-based ecological carrying capacity dataset of the Guangdong-Hong Kong- Macao Greater Bay Area (1990–2019)
Dataset short name	GBA_SSECC_1990_2019
Authors	Wang, M. D. JOK-0331-2023, MNR Key Laboratory for Geo-Environmental Monitoring of Great Bay Area & Guangdong–Hong Kong-Macau Joint Laboratory for Smart Cities & State Key Labora-tory of Subtropical Building and Urban Science, Shenzhen University, wangmengdi2020@ email.szu.edu.cn Tang, Y. Z. DVW-4921-2022, Guangdong Laboratory of Artificial Intelligence and Digital Economy (SZ), tangyuzhi@gml.ac.cn Shi, T. Z., GBX-5637-2022, MNR Key Laboratory for Geo-Environmental Monitoring of Great Bay Area & Guangdong–Hong Kong-Macau Joint Laboratory for Smart Cities & State Key Labora-tory of Subtropical Building and Urban Science, Shenzhen University,tiezhushi@szu.edu.cn Liu, Q. JOK-0735-2023, Department of Land Surveying and Geomatics, The Hong Kong Polytechnic University, qian999.liu@polyu.edu.hk Yan, F. Q. HGN-6431-2022, State Key Laboratory of Resources and Environmental Information System, Institute of Geographic Sciences and Natural Resources Research, yanfq@ lreis.ac.cn Lv, P. JOK-0446-2023, MNR Key Laboratory for Geo-Environmental Monitoring of Great Bay Area & Guangdong–Hong Kong-Macau Joint Laboratory for Smart Cities & State Key Labora-tory of Subtropical Building and Urban Science, Shenzhen University, 2100432095@ email.szu.edu.cn Deng, D. P. JOK-0582-2023, MNR Key Laboratory for Geo-Environmental Monitoring of Great Bay Area & Guangdong–Hong Kong-Macau Joint Laboratory for Smart Cities & State Key Labora-tory of Subtropical Building and Urban Science, Shenzhen University, dengdong-ping 2021@email.szu.edu.cn Zhang, Z. H. HDN-8369-2022, MNR Key Laboratory for Geo-Environmental Monitoring of Great Bay Area & Guangdong–Hong Kong-Macau Joint Laboratory for Smart Cities & State Key Labora-tory of Subtropical Building and Urban Science, Shenzhen University, 2200325014@ email.szu.edu.cn Wang, Z. H. HIF-7028-2022, State Key Laboratory of Resources and Environmental Information System, Institute of Geographic Sciences and Natural Resources Research, wang@lreis.ac.cn Wu, G. F. B-8735-2018, MNR Key Laboratory for Geo-Environmental Monitoring of Great Bay Area & Guangdong–Hong Kong-Macau Joint Laboratory for Smart Cities & State Key Labora- tory of Subtropical Building and Urban Science, Shenzhen University, guofeng.wu@szu.edu.cn Su, F. Z. DXY-6694-2022, State Key Laboratory of Resources and Environmental Information System, Institute of Geographic Sciences and Natural Resources Research, CAS, sufz@lreis.ac.cn
Geographical region	Coastal zones and marine areas of the Greater Bay Area of Guangdong, Hong Kong and Macao
Year	1990–2019
Temporal resolution	10 year
Spatial resolution	30 m
Data format	.xlsx, .tif, .shp
Data size	8.97 MB (Compressed)
Data files	Spatial scene distribution maps of coastal zone and sea area in Guangdong, Hong Kong, Macao and the Greater Bay Area for 1990, 2000, 2010, and 2019 (.tif format, 32 files in total); coastal zone of Guangdong, Hong Kong, Macao and the Greater Bay Area from 1990–2019 (.shp format, 24 files in total); scene conversion between sea, land, and air from 1990–2019 (.xlsx format, 1 file); ecological carrying capacity and ecological footprint results of the study area, 1990–2019 (.xlsx format, 1 file)
Foundations	National Natural Science Foundation of China (42306245, 41890854); Department of Science and Technology of Guangdong Province (2020B1212030009)
Data publisher	Global Change Research Data Publishing & Repository, http://www.geodoi.ac.cn
Address	No. 11A, Datun Road, Chaoyang District, Beijing 100101, China
Data sharing policy	(1) *Data* are openly available and can be free downloaded via the Internet; (2) End users are encouraged to use *Data* subject to citation; (3) Users, who are by definition also value-added service providers, are welcome to redistribute *Data* subject to written permission from the GCdataPR Editorial Office and the issuance of a *Data* redistribution license; and (4) If *Data* are used to compile new datasets, the 'ten per cent principal' should be followed such that *Data* records utilized should not surpass 10% of the new dataset contents, while sources should be clearly noted in suitable places in the new dataset[10]
Communication and searchable system	DOI, CSTR, Crossref, DCI, CSCD, CNKI, SciEngine, WDS, GEOSS, PubScholar, CKRSC

wetlands, and artificial scenes based on land cover characteristics and ecological functions. These major types were further subdivided according to their socio-economic attributes and ecological impact. Forest land, for instance, was differentiated into ecologically protected forests and economically oriented plantations. Water bodies and wetlands encompassed open freshwater areas, aquaculture ponds, and wetlands with significant ecological regulatory functions. Artificial scenes, being more complex, included residential areas, public service facilities, commercial areas, industrial production zones, as well as transportation logistics and energy facilities.

The remote sensing data utilized for spatial scene classification in the study area comprised Landsat images covering the research area for 1990, 2000, 2010, and 2019, obtained through the Google Earth Engine platform. Landsat employs high-resolution multispectral sensors with 11 spectral bands, all possessing relatively high spatial resolution. The commonly used visible and near-infrared bands have a resolution of 30 m. Images of the same area can be acquired every 16 days, providing high temporal resolution. To ensure data quality and accuracy, this study employed TOA (Top of Atmosphere) product data, which had already undergone cloud removal processing.

Statistical data on biological resources and energy consumption in the study area were primarily sourced from the Guangdong Provincial Statistical Yearbook (1990–2020)[15–18] and statistical yearbooks of the 9 cities involved in the study area (1990–2020)[19–46][1]. This was supplemented by the Guangdong Rural Statistical Yearbook (1990–2020)[47–50], various Chinese statistical yearbooks on energy, transportation, fisheries, oceans, automotive industry, electricity, and cities[51–78], as well as survey reports from local governments, regulatory departments, industries, and enterprises, and city and county yearbooks or chronicles. Based on the study area's actual situation and the 27 spatial scenes and 6 land types classified, account data for different spatial scenes and land types was summarized and analyzed. The biological resource account primarily utilized production data for agricultural, forestry, grassland, and aquatic products as the assessment basis. The energy consumption account focused mainly on industrial energy consumption and electricity[79]. Relevant cities' resident population data were collected to obtain per capita consumption in the study area. Global per capita consumption data were derived from the "2020 World Food and Agriculture Statistical Yearbook"[80] published by the Food and Agriculture Organization of the United Nations[2]. This data comprehensively introduces the main factors in the current global food and agriculture field, covering about 20,000 indicators for 245 countries and regions, providing key facts and trends in food and agriculture. Vegetation Net Primary Production (NPP) data were sourced from MODIS products[81] (for land) and VGPM products[82] (for marine areas). Coastal resident population data were primarily derived from statistical yearbooks and WorldPop spatial population distribution data[3]. Data on car ownership by vehicle type and energy type were primarily purchased from automotive industry companies. Annual ship traffic density maps for the Pearl River Estuary were sourced from Marine Traffic[4], and spatial distribution data of marine aquaculture in the Greater Bay Area were obtained from Liu *et al*.[83]. Additionally, necessary parameters were acquired from published literature, data platform searches, and news reports.

---

[1] Statistical data for Hong Kong are from the Census and Statistics Department of the Hong Kong Special Administrative Region Government website: https://www.censtatd.gov.hk/tc/page_1226.html; Statistical data for Macau are from the Statistics and Census Service of the Macau Special Administrative Region Government website: https://www.dsec.gov.mo/zh-MO/Statistic/Database.

[2] Data is from the Food and Agriculture Organization of the United Nations (FAO) official website. http://www. fao.org/.

[3] Data is from the WorldPop official website. https://www.worldpop.org/.

[4] Data are from the Marine Traffic official website. www.marinetraffic.com.

3.1 Algorithmic Principles

3.1.1 Spatial Scene Classification and Extraction Methodology

The classification of spatial scenes presents a more nuanced approach compared to traditional land cover types. Due to the spectral similarity of most artificial scenes, direct remote sensing classification is often challenging and potentially less accurate. To address this issue, a classification strategy combining remote sensing data with socially perceived data was implemented (Figure 1).

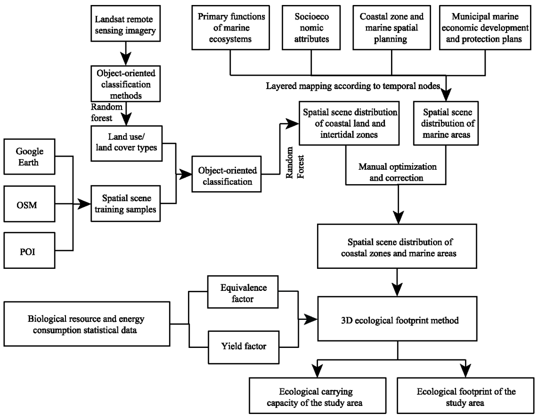

Figure 1 Technical flow chart of dataset development

Initially, the Object-Based Image Classification (OBIC) method, in conjunction with the Random Forest algorithm on the SuperSIAT 2.1 platform[84,85], was employed to identify and classify six Land Use/Land Cover (LULC) types from Landsat remote sensing imagery. These types include forest, grassland, cropland, water bodies, artificial land, and bare land. Subsequently, feature extraction was conducted by integrating OpenStreetMap (OSM), Google Earth imagery, Point of Interest (POI) data, and remote sensing influence data to generate spatial scene training samples (70%). These samples provided essential reference information about various spatial scenes, offering valuable auxiliary data for the classification process and further refining the classification results.

Following the sample generation, the SuperSIAT 2.1 platform was utilized to further subdivide land cover types into specific related spatial scenes based on the spatial scene training samples and the Random Forest algorithm. This process completed the spatial scene mapping of coastal land and intertidal zones. For instance, forest land was subdivided into forests and plantations, while artificial land was categorized into residential areas, commercial and trade zones, industrial production areas, public service areas, and rail and road bridges, among others. A more detailed classification of different land cover types was conducted based on the texture features and spectral information of spatial scenes, as well as semantic features extracted from socially perceived data.

Concurrently, marine spatial scenes were overlaid and integrated with coastal land and intertidal spatial scenes, guided by relevant policies and following temporal nodes. Due to this integration, the preliminary spatial scene classification results were obtained. The last stage was refining the results of the described preliminary classification by performing a manual visual inspection to ensure accuracy and reliability.

3.1.2 Estimation of Coastal and Marine Ecological Carrying Capacity Based on the Three-Dimensional Ecological Footprint Model

The ecological capacity of the study area was estimated using an algorithm of biological resources and energy consumption combined with the Net Primary Productivity (NPP) for the period of 1990–2019. These data were used to set up the equivalence factors, the yield factors, incorporate product categories, and generate information for every spatial scene. In the next step, the three-dimensional ecological footprint model was used to compute footprints' features, including footprint breadth and depth, ecological carrying capacity, and ecological deficit for each spatial scene and the whole study area.

The MOD173AH annual NPP data is the basic summation of the annual net photosynthesis (PSN) estimated from the 8-day composites of the MOD17A2H product. PSN values are obtained from the difference between the Gross Primary Productivity (GPP) and the Maintenance Respiration (MR). Spatial and temporal data resolutions of the dataset are 500 m and one year, respectively. The research area covers the image tile h28v06. The data from the years 1990, 2000, 2010, and 2019 were obtained and then pre-processed by applying operations such as projection transformation, resampling, averaging, and cropping.

(1) Calculation of equivalence factors and yield factors

The equivalence factors r_i and yield factors y_i were primarily assessed using the Net Primary Productivity (NPP) method, as referenced by Liu et al.[86] . The calculation equations are as follows:

$$r_i = \frac{\text{NPP}_{i,\ local}}{\text{NPP}_{local}} \tag{1}$$

$$y_i = \frac{\text{NPP}_{i,\ local}}{\text{NPP}_{i,\ global}} \tag{2}$$

where, $\text{NPP}_{i,\ local}$, NPP_{local} , and $\text{NPP}_{i,\ global}$ are the average NPP of a certain spatial scene or land type in the study area, the average NPP of the whole study area, and the global average NPP of a certain spatial scene or land type, respectively. At the same time, there is no global-scale spatial scene distribution data, which limits the ability to derive the global average NPP from spatial scenes. Nevertheless, there is more information on global land use/land cover, which enables the estimation of the average NPP by land type. An approximate calculation of global average NPP values based on spatial scenes can be obtained using the following equation: an approximate calculation of global average NPP values based on spatial scenes can be obtained using the following equation:

$$\text{NPP}_{i,\ global} = \frac{\text{NPP}_{i,\ local}}{\text{NPP}_{i_{land},\ local}} \times \text{NPP}_{i_{land},\ global} \tag{3}$$

where, $\text{NPP}_{i_{land},\ local}$ and $\text{NPP}_{i_{land},\ global}$ represent the average NPP values of the land type corresponding to a specific spatial scene in the study area and globally, respectively.

(2) Calculation of ecological carrying capacity indicators based on the three-dimensional ecological footprint

The three-dimensional ecological footprint model defines two new indicators—the footprint depth, which reflects the extent of destruction of natural capital stock, and the footprint breadth, which shows the degree of human activity's consumption of natural capital flow[87,88]. This is deemed more scientifically correct and realistic as compared to the conventional ecological footprint model. The calculation equation is as follows:

$$EF_{\text{3D}} = EF_{\text{size}} \times EF_{\text{depth}} \tag{4}$$

where, EF_{3D} represents the three-dimensional ecological footprint; EF_{size} represents the ecological footprint breadth; and EF_{depth} represents the ecological footprint depth. The current three-dimensional ecological footprint model is primarily based on six land types:

cropland, forest land, grassland, fishing grounds, built-up land, and energy land. For each land type, the model determines the equivalence factors, yield factors, account product categories, and data. Subsequently, the footprint breadth, footprint depth, ecological carrying capacity, and ecological deficit are assessed for each land type and the region as a whole.

3.2 Methodological Framework

The methodological framework employed in this study is depicted in Figure 1. Multiple data sources were utilized, including Landsat remote sensing imagery, Google Earth, OpenStreetMap (OSM), and Points of Interest (POI). An object-oriented classification method incorporating the Random Forest algorithm was implemented to complete the spatial scene classification of coastal land and intertidal zones within the study area. Concurrently, the distribution of marine spatial scenes in the study area was determined through the integration of several factors: the primary functions of marine ecosystems, socio-economic attributes, coastal and marine spatial planning, and marine economic development protection plans of various cities within the study area. These factors were overlaid according to temporal nodes and subsequently merged to generate a comprehensive dataset of spatial scene distribution in the coastal zone and marine areas of the study area.

In parallel, the study area's equivalence factors and yield factors were calculated based on biological resource and energy consumption statistical data from the region. Subsequently, utilizing the spatial scene distribution of the study area, the three-dimensional ecological footprint method was applied to quantify the ecological carrying capacity and ecological footprint within the study area.

4 Data Results and Validation

4.1 Data Composition

The dataset is comprised of four distinct data files:

(1) Spatial scenes distribution dataset of the coastal zone and marine areas in the Guangdong-Hong Kong-Macao Greater Bay Area:

This dataset is provided in .tif format and contains spatial scene distribution maps of the study area for the years 1990, 2000, 2010, and 2019.

(2) Ecological carrying capacity and ecological footprint data for the coastal zone and marine areas in the Guangdong-Hong Kong-Macao Greater Bay Area:

Archived in .xlsx format, this dataset encompasses comprehensive calculations for the study area from 1990 to 2019. The data includes: total ecological carrying capacity; per capita ecological carrying capacity; ecological footprint breadth; ecological footprint depth; and 3D ecological footprint results for various spatial scenes.

(3) Coastline dataset of the Guangdong-Hong Kong-Macao Greater Bay Area from 1990 to 2019:

This dataset is provided in .shp format and features coastline distribution maps of the Guangdong-Hong Kong-Macao Greater Bay Area for the years 1990, 2000, 2010, and 2019.

(4) Land-sea transition data for the coastal zone and marine areas in the Guangdong-Hong Kong-Macao Greater Bay Area:

Archived in .xlsx format, this dataset illustrates the coastal zone changes within the study area, providing a comprehensive overview of the land-sea transition status in the research region.

4.2 Data Products

4.2.1 Spatiotemporal Distribution Results of Spatial Scenes

The spatiotemporal distribution of scenes in the study area from 1990 to 2019 is depicted in

Figure 2[14]. Over the past three decades, significant transformations have been observed in both terrestrial and intertidal zones. Forests and paddy fields have predominantly been converted into various spatial scenes, including marine aquaculture, residential areas, commercial and trade zones, industrial production areas, and rail and road bridges. The most intense period of this conversion was observed during the initial two decades of the study period.

In marine areas, a notable transition has been identified from development reserve areas and general fishing grounds to marine protected areas, marine aquaculture, tourism and leisure zones, port channels, and industrial urban marine areas. A particularly significant bidirectional conversion between development reserve areas and marine aquaculture zones was observed between 2010 and 2019.

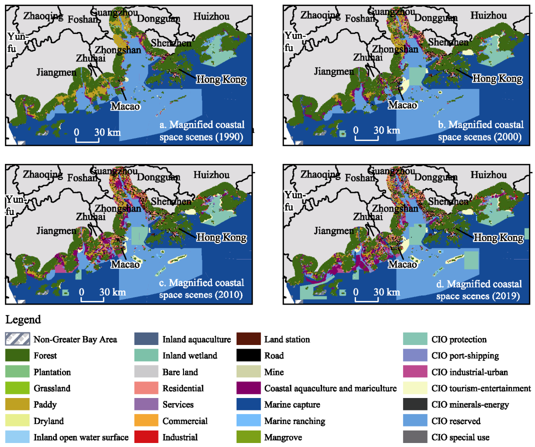

Figure 2 Spatiotemporal distribution maps of spatial scenes in terrestrial and intertidal zones of the Greater Bay Area (1990–2019)

4.2.2 Ecological Carrying Capacity and Ecological Footprint Results

Table 2 presents the ecological carrying capacity results for the study area from 1990 to 2019. The total ecological carrying capacity of the study area exhibited an initial increase followed by a subsequent decrease over the 1990–2019 period. Concurrently, the per capita ecological carrying capacity demonstrated an overall downward trend, with an accelerated rate of decline observed post-2000. With the exception of paddy fields and marine development reserve areas, the total ecological carrying capacity of all other spatial scenes generally exhibited an upward trend. The spatial scenes exhibiting the highest annual per capita ecological carrying capacity were identified as general fishing grounds, marine development reserve areas, forests, and marine aquaculture. It is noteworthy that the substantial decrease in the per capita ecological carrying capacity of general fishing grounds was identified as the primary factor contributing to the overall decline in regional per capita ecological carrying capacity.

Table 3 illustrates the evolution of the ecological footprint in the study area from 1990 to 2019. The per capita ecological footprint breadth demonstrated an upward trend from 1990 to 2000, followed by a slight decline post-2000, exhibiting an overall gentle change trend. This trend was primarily influenced by paddy fields and general fishing grounds. The vast majority of spatial scenes demonstrated an overall upward trend, albeit with low annual average growth rates.

The per capita 3D ecological footprint consistently increased from 3.03 to 10.54, consistently exceeding the critical value of 1, indicating a trend of unsustainable regional development. The footprint depth for most spatial scenes exceeded 1 across all years, suggesting a current state of unsustainable development for the majority of spatial scenes. The per capita 3D ecological footprint exhibited a trend characterized by a rapid initial increase followed by a more gradual increase. This trend was primarily associated with the rapid growth of the forest's 3D footprint. Most spatial scenes exhibited an overall upward trend in per capita 3D footprint. Only paddy fields, dry land, open freshwater areas, and freshwater aquaculture pond scenes demonstrated a declining trend in per capita 3D ecological footprint.

Table 2 Total ecological carrying capacity and per capita ecological carrying capacity of the Greater Bay Area's coastal zone and marine areas (1990–2019)

Spatial scene	Total ecological carrying capacity (10^4 hm^2)				Per capita ecological carrying capacity (hm^2/10^4 person)			
	1990	2000	2010	2019	1990	2000	2010	2019
Forest	18.00	17.55	36.70	48.21	193.94	114.29	193.12	219.18
Plantation	0.16	0.29	0.16	0.46	1.70	1.92	0.83	2.07
Grassland	0.11	0.84	1.72	3.40	1.21	5.49	9.06	15.44
Paddy	31.01	14.54	12.84	11.67	334.07	94.70	67.58	53.07
Dryland	0.15	0.59	0.16	0.34	1.58	3.83	0.83	1.55
Inland open water surface	0.28	0.60	0.87	0.93	3.04	3.89	4.60	4.24
Inland aquaculture	0.04	1.07	0.15	0.26	0.43	6.96	0.80	1.20
Inland wetland	0.00	0.04	0.00	0.01	0.04	0.23	0.02	0.05
Bare land	0.00	0.00	0.00	0.00	0.00	0.00	0.00	0.00
Residential	2.85	6.38	8.44	11.00	30.72	41.54	44.40	50.00
Services	0.03	0.05	0.09	1.14	0.33	0.33	0.46	5.18
Commercial	0.45	3.55	6.21	11.13	4.87	23.12	32.68	50.62
Industrial	0.77	2.92	4.67	8.72	8.24	19.01	24.55	39.65
Land station	0.07	0.35	0.43	0.80	0.75	2.29	2.25	3.62
Road	1.67	3.96	4.32	6.36	17.98	25.81	22.74	28.92
Mine	0.00	0.00	0.00	0.01	0.01	0.01	0.01	0.03
Mangrove	0.01	0.01	0.06	0.05	0.07	0.07	0.32	0.24
Coastal aquaculture and mariculture	1.87	24.24	46.16	46.17	20.18	157.89	242.92	209.89
Marine capture	467.73	745.07	657.71	515.58	5,038.62	4,853.48	3,461.47	2,344.01
Marine ranching	0.00	0.00	0.21	0.50	0.00	0.00	1.10	2.25
CIO protection	2.96	7.93	7.67	11.45	31.86	51.69	40.38	52.06
CIO port-shipping	2.15	3.89	4.56	3.92	23.13	25.37	24.00	17.83
CIO industrial-urban	0.02	0.10	1.74	1.36	0.19	0.64	9.14	6.19
CIO tourism-entertainment	0.26	2.34	2.66	2.44	2.77	15.23	14.00	11.07
CIO minerals-energy	16.76	26.75	23.65	18.68	180.60	174.25	124.45	84.91
CIO reserved	34.59	48.49	38.78	27.66	372.61	315.86	204.08	125.74
CIO special use	0.03	0.05	0.05	0.04	0.37	0.35	0.25	0.17
Total	581.97	911.60	859.99	732.27	6,269.30	5,938.25	4,526.07	3,329.17

4.2.3 Dynamic Results of Land-Sea Transition in Spatial Scenes

The dataset extracted coastlines from 1990 to 2019 based on spatial scene classification results, as depicted in Figure 3[14]. Over the past three decades, significant changes in the study area's coastline have been observed, primarily characterized by seaward extension. The most pronounced coastline changes occurred during the 1990–2000 period, particularly along the Pearl River Estuary. Post-2010, the rate of coastline extension towards the sea exhibited signs of deceleration.

Figure 4 illustrates the land-sea spatial scene transitions from 1990 to 2019. The primary trend during this period was identified as the conversion of development reserve areas and general fishing grounds into other spatial scenes. This transformation was particularly evident between 1990 and 2010, characterized by extensive transitions from marine to terrestrial scenes.

Table 3 Changes in per capita footprint breadth, footprint depth, and 3D footprint of the Greater Bay Area's coastal zone and marine areas (1990–2019)

Spatial scene	Per capita footprint breadth ($hm^2/10^4$ person)				Per capita footprint depth				Per capita 3D footprint ($hm^2/10^4$ person)			
	1990	2000	2010	2019	1990	2000	2010	2019	1990	2000	2010	2019
Forest	193.94	114.29	193.12	219.18	18.46	85.39	94.25	74.82	3,579.37	9,759.44	1,8201.10	16,399.21
Plantation	1.70	1.92	0.83	2.07	82.62	135.70	307.77	137.90	140.09	259.88	255.31	285.77
Grassland	1.21	5.49	9.06	15.44	623.44	161.78	109.13	107.96	751.84	888.08	988.34	1,667.25
Paddy	334.07	94.70	67.58	53.07	3.65	7.32	6.19	9.91	1,219.64	692.75	418.20	525.81
Dryland	1.58	3.83	0.83	1.55	455.58	278.52	798.17	421.01	719.47	1,065.85	661.96	653.17
Inland open water surface	3.04	3.89	4.60	4.24	44.83	20.02	12.60	12.67	136.18	77.91	58.03	53.74
Inland aquaculture	0.43	6.96	0.80	1.20	146.89	6.73	38.42	23.16	63.19	46.88	30.63	27.69
Residential	30.72	41.54	44.40	50.00	14.50	10.06	13.49	16.93	445.40	417.76	599.07	846.81
Services	0.33	0.33	0.46	5.18	69.38	365.74	309.19	48.89	22.82	121.74	141.94	253.08
Commercial	4.87	23.12	32.68	50.62	8.76	8.47	10.20	11.54	42.63	195.75	333.24	584.26
Industrial	8.24	19.01	24.55	39.65	587.45	338.51	364.69	191.28	4,842.44	6,433.98	8,953.83	7,583.52
Land station	0.75	2.29	2.25	3.62	663.29	189.91	544.72	499.80	499.72	434.84	1,227.21	1,810.55
Road	17.98	25.81	22.74	28.92	40.29	42.67	76.32	31.16	724.45	1,101.39	1,735.62	901.12
Mine	0.01	0.01	0.01	0.03	21.51	58.67	324.16	30.15	0.21	0.39	2.62	0.76
Coastal aquaculture and mariculture	9.46	15.79	14.75	12.57	1.00	1.00	1.00	1.00	9.46	15.79	14.75	12.57
Marine capture	2,462.08	3,183.31	2,940.16	2,344.01	1.00	1.00	1.00	1.17	2,462.08	3,183.31	2,940.16	2,735.15
CIO port-shipping	23.13	25.37	24.00	17.83	6.31	3.81	7.17	15.59	146.00	96.74	172.11	277.88
CIO industrial-urban	0.19	0.64	4.23	6.19	62.25	8.01	1.00	1.18	11.55	5.16	4.23	7.32
CIO tourism-entertainment	0.44	0.30	0.16	0.09	1.00	1.00	1.00	1.00	0.44	0.30	0.16	0.09
CIO minerals-energy	0.06	3.79	2.92	4.89	1.00	1.00	1.00	1.00	0.06	3.79	2.92	4.89
Total	3,094.21	3,572.39	3,390.14	2,860.33	3.03	4.58	8.37	10.54	9,373.54	16,343.71	28,371.11	30,156.50

Note: The ecological footprint calculations temporarily exclude certain categories of data due to unavailability or inapplicability. Specifically, detailed biological resource output data for freshwater wetlands and marine ranches are not accessible. Mangrove forests and marine protected areas, being conservation zones, do not engage in production activities. Energy consumption data for development reserve sea areas and special-use sea areas are unobtainable. Additionally, bare land produces no output. Consequently, these data categories have been omitted from the current ecological footprint calculations.

However, post-2010, the dominant feature shifted to reciprocal conversions between land and sea scenes, accompanied by a significant reduction in human expansion into marine areas. This shift suggests a gradual move towards a more balanced approach in marine resource exploitation and a decrease in human impact on the marine environment in recent years.

The sustainability changes resulting from land-sea transitions were calculated by multiplying the areas of transitional spatial scenes from 1990 to 2019 with their respective ecological carrying capacities and ecological footprints before and after conversion (Figure 5). Research findings indicate an increasing trend in the ecological carrying capacity of land-sea transitional areas across all periods. Terrestrial scenes demonstrated significantly higher unit ecological footprints compared to marine scenes. Additionally, the deceleration of marine-to-terrestrial conversion in the past decade has led to a slight decrease in the ecological deficit caused by land-sea transitions.

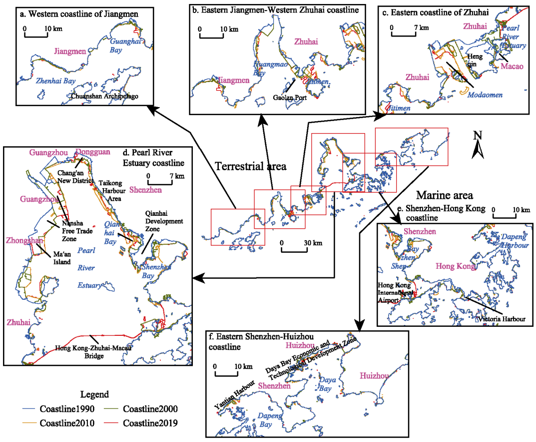

Figure 3 Spatiotemporal dynamics map of the Greater Bay Area coastline (1990–2019)

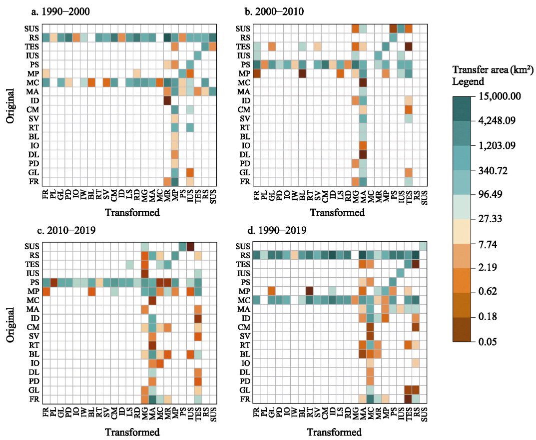

Figure 4 Map of land-sea spatial scene transitions in the Greater Bay Area (1990–2019)

4.3 Data Validation

To verify the accuracy of the spatial scene classification results, accuracy assessments were conducted for each period's classification outcomes. The validation results demonstrate that the overall accuracies of spatial scene classification for 1990, 2000, 2010, and 2019 reached 85.10%, 82.72%, 80.19%, and 80.65%, respectively. These accuracy levels are deemed sufficient to meet the requirements of the research.

5 Discussion and Conclusion

The ecological carrying capacity estimation method based on spatial scenes is an assessment approach that incorporates geographical spatial characteristics and local environmental conditions[10]. This approach combines the use of GIS and spatial analysis with the Ecological Footprint model, enabling more accurate estimation of the ecosystem's carrying capacity within specific geographical ranges. This method fully reflecting the main sources and micro-composition of regional ecological carrying capacity and ecological footprint, this approach aids in elucidating the causes of regional sustainability changes and supports evidence-based decision-making.

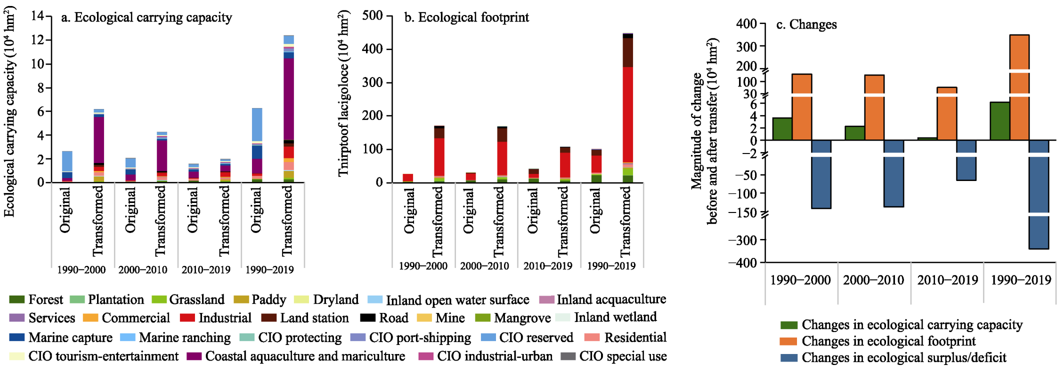

Figure 5 Comparison of (a) ecological carrying capacity, (b)ecological footprint, and (c) the changes before and after spatial scene conversion in the land-sea transition areas of the Greater Bay Area (1990–2019)

The development methodology of this dataset maximizes the utilization of multi-source data. Classification methods based on the object-oriented paradigm are used to provide accurate results for the classification of spatial scenes in the study area. These classifications are then integrated with three dimensional ecological footprint estimations in order to measure ecological carrying capacity and ecological footprint from 1990 to 2019.

The data results reveal the trends in ecological carrying capacity and sustainability of the Guangdong-Hong Kong-Macao Greater Bay Area over the past 30 years, and highlight potential ecological and environmental issues. The first general trend of spatial scene dynamic changes is the conversion from natural and agricultural land into urban and artificial space. On the other hand, the use of marine utilization shows trends towards diversification and protection orientation. These patterns reflect the evolution of spatial scene utilization pressure and marine resource management policies during the region's rapid development process.

The ecological footprint and ecological carrying capacity data in this dataset reveal that terrestrial scenes have significantly higher unit ecological footprints compared to marine areas. However, the ecological carrying capacity of land-sea transitional areas has continuously increased. Furthermore, the trend of marine-to-terrestrial conversion has decelerated in the past decade. This deceleration has led to a slight decrease in the ecological deficit caused by land-sea transitions, indicating an improvement in the ecological and environmental conditions of the study area.

The overall accuracy of classification results for all four stages in this dataset exceeds 80%, with the 1990 spatial scene classification achieving the highest accuracy at 85.10%. Consequently, this dataset demonstrates considerable potential for providing robust support for future coastal ecological protection and integrated management. It offers a scientific foundation for formulating coastal sustainable development strategies and informed decision-making processes.

Author Contributions

The dataset development was comprehensively designed by Tang, Y. Z., Shi, T. Z., and Su, F. Z. Sample data and remote sensing imagery were collected and processed by Wang, M. D. and Liu, Q. Biological resource and energy consumption data were gathered and processed by Wang, M. D., Lv, P., Deng, D. P., Zhang, Z. H., and Wang, Z. H. The models and algorithms were designed by Tang, Y. Z. The data validation was performed by Liu, Q. and Wang, M. D. The data paper was authored by Wang, M. D. and Tang, Y. Z. Guidance and revisions to the paper were provided by Shi, T. Z., Yan, F. Q., Hu, Z. W., and Wu, G. F.

Conflicts of Interest

The authors declare no conflicts of interest.

References

[1] Neumann, B., Ott, K., Kenchington, R. Strong sustainability in coastal areas: a conceptual interpretation of SDG 14 [J]. *Sustainability science*, 2017, 12: 1019–1035.

[2] Ye, G., Chou, L. M., Yang, S., *et al*. Is integrated coastal management an effective framework for promoting coastal sustainability in China's coastal cities? [J]. *Marine Policy*, 2015, 56: 48–55.

[3] McKinley, E., Acott, T., Yates, K. L. Marine social sciences: Looking towards a sustainable future [J]. *Environmental Science* & *Policy*, 2020, 108: 85–92.

[4] Zhao, W., Zhao, G., Yang, J., *et al*. Assessment of the ecological security of the coastal zone of the Guangdong/Hong Kong/Macao Greater Bay area [J]. *Journal of Coastal Research*, 2020, 102(SI): 287–295.

[5] Yang, C., Gan, H., Wan, R., *et al*. Spatiotemporal evolution and influencing factors of coastline in the Guangdong-Hong Kong-Macao Greater Bay Area from 1975 to 2018 [J]. *China Geology*, 2021, 48(3): 697–707.

[6] Zhao, M. M., Kou, J. F., Yang, J., *et al*. Study on the ecological security and protection measures of the coastal zone in Guangdong-Hong Kong-Macao Greater Bay Area [J]. *Environmental Protection*, 2019, 47(23): 29–34.

[7] Zhai, T., Wang, J., Fang, Y., *et al*. Assessing ecological risks caused by human activities in rapid urbanization coastal areas: towards an integrated approach to determining key areas of terrestrial-oceanic ecosystems preservation and restoration [J]. *Science of the Total Environment*, 2020, 708: 135153.

[8] Guan, D. M., Zhang, Z. F., Yang, Z. X., *et al*. Research on measuring strategy of carrying capacity of marine resources and environment [J]. *Bulletin of Chinese Academy of Sciences*, 2016, 31(10): 1241–1247

[9] Wang, M. D., Tang, Y. Z., Shi, T. Z., *et al*. Spatial scenes-based ecological carrying capacity dataset for the Guangdong-Hong Kong-Macao Greater Bay Area (1990–2019) [J/DB/OL]. *Digital Journal of Global Change Data Repository*, 2024. https://doi.org/10.3974/geodb.2024.06.03.V1. https://cstr.escience.org.cn/CSTR:20146.11.2024.06.03.V1.

[10] GCdataPR Editorial Office. GCdataPR data sharing policy [OL]. https://doi.org/10.3974/dp.policy.2014.05 (Updated 2017).

[11] Technical Steering Group for the National Comprehensive Survey of Coastal Zone and Mudflat Resources. Comprehensive Survey of Coastal Zone and Mudflat Resources in China (Illustration Collection) [M]. Beijing: Ocean Publishing House, 1991.

[12] Nordquist, M. H., Nandan, S. N., Kraska, J. United Nations Convention on the Law of the Sea 1982, Volume VII: a Commentary [M]. Martinus Nijhoff Publishers, 2011.

[13] National marine functional zoning (2011–2020) [N]. China Marine, 2012-04-18 (005), special edition.

[14] Tang, Y. Z., Shi, T. Z., Liu, Q., *et al*. Ecological carrying capacity and sustainability assessment for coastal and maritime area based on spatial scene: a case study of the Guangdong-Hong Kong-Macao Greater Bay Area [J]. *Acta Geographica Sinica*, 2023, 78(11): 2811–2832.

[15] Bureau, Guangdong Province Statistical. Statistical yearbook of Guangdong Province 1990 [M]. Beijing: China Statistics Press, 1991.

[16] Bureau, Guangdong Province Statistical. Statistical yearbook of Guangdong Province 2000 [M]. Beijing: China Statistics Press, 2001.

[17] Bureau, Guangdong Province Statistical. Statistical yearbook of Guangdong Province 2010 [M]. Beijing: China Statistics Press, 2011.

[18] Bureau, Guangdong Province Statistical. Statistical yearbook of Guangdong Province 2019 [M]. Beijing: China Statistics Press, 2020.

[19] Shenzhen Bureau of Statistics. Statistical Yearbook of Shenzhen 1990 [M]. Beijing: China Statistics Press, 1991.

[20] Shenzhen Bureau of Statistics. Statistical Yearbook of Shenzhen 2000 [M]. Beijing: China Statistics Press, 2001.

[21] Shenzhen Bureau of Statistics. Statistical Yearbook of Shenzhen 2010 [M]. Beijing: China Statistics Press, 2011.

[22] Shenzhen Bureau of Statistics. Statistical Yearbook of Shenzhen 2019 [M]. Beijing: China Statistics Press, 2020.

[23] Dongguan Bureau of Statistics. Statistical Yearbook of Dongguan 1990 [M]. Beijing: China Statistics Press, 1991.

[24] Dongguan Bureau of Statistics. Statistical Yearbook of Dongguan 2000 [M]. Beijing: China Statistics Press, 2001.

[25] Dongguan Bureau of Statistics. Statistical Yearbook of Dongguan 2010 [M]. Beijing: China Statistics Press, 2011.

[26] Dongguan Bureau of Statistics. Statistical Yearbook of Dongguan 2019 [M]. Beijing: China Statistics Press, 2020.

[27] Huizhou Bureau of Statistics. Statistical Yearbook of Huizhou 1990 [M]. Beijing: China Statistics Press, 1991.

[28] Huizhou Bureau of Statistics. Statistical Yearbook of Huizhou 2000 [M]. Beijing: China Statistics Press, 2001.
[29] Huizhou Bureau of Statistics. Statistical Yearbook of Huizhou 2010 [M]. Beijing: China Statistics Press, 2011.
[30] Huizhou Bureau of Statistics. Statistical Yearbook of Huizhou 2019 [M]. Beijing: China Statistics Press, 2020.
[31] Zhongshan Bureau of Statistics. Statistical Yearbook of Zhongshan 1990 [M]. Beijing: China Statistics Press, 1991.
[32] Zhongshan Bureau of Statistics. Statistical Yearbook of Zhongshan 2000 [M]. Beijing: China Statistics Press, 2001.
[33] Zhongshan Bureau of Statistics. Statistical Yearbook of Zhongshan 2010 [M]. Beijing: China Statistics Press, 2011.
[34] Zhongshan Bureau of Statistics. Statistical Yearbook of Zhongshan 2019 [M]. Beijing: China Statistics Press, 2020.
[35] Guangzhou Bureau of Statistics. Statistical Yearbook of Guangzhou 1990 [M]. Beijing: China Statistics Press, 1991.
[36] Guangzhou Bureau of Statistics. Statistical Yearbook of Guangzhou 2000 [M]. Beijing: China Statistics Press, 2001.
[37] Guangzhou Bureau of Statistics. Statistical Yearbook of Guangzhou 2010 [M]. Beijing: China Statistics Press, 2011.
[38] Guangzhou Bureau of Statistics. Statistical Yearbook of Guangzhou 2019 [M]. Beijing: China Statistics Press, 2020.
[39] Zhuhai Bureau of Statistics. Statistical Yearbook of Zhuhai 1990 [M]. Beijing: China Statistics Press, 1991.
[40] Zhuhai Bureau of Statistics. Statistical Yearbook of Zhuhai 2000 [M]. Beijing: China Statistics Press, 2001.
[41] Zhuhai Bureau of Statistics. Statistical Yearbook of Zhuhai 2010 [M]. Beijing: China Statistics Press, 2011.
[42] Zhuhai Bureau of Statistics. Statistical Yearbook of Zhuhai 2019 [M]. Beijing: China Statistics Press, 2020.
[43] Jiangmen Bureau of Statistics. Statistical Yearbook of Jiangmen 1990 [M]. Beijing: China Statistics Press, 1991.
[44] Jiangmen Bureau of Statistics. Statistical Yearbook of Jiangmen 2000 [M]. Beijing: China Statistics Press, 2001.
[45] Jiangmen Bureau of Statistics. Statistical Yearbook of Jiangmen 2010 [M]. Beijing: China Statistics Press, 2011.
[46] Jiangmen Bureau of Statistics. Statistical Yearbook of Jiangmen 2019 [M]. Beijing: China Statistics Press, 2020.
[47] Editorial Committee of the Guangdong Rural Statistics Yearbook. Guangdong Rural Statistics Yearbook 1990 [M]. Beijing: China Statistics Press, 1991.
[48] Editorial Committee of the Guangdong Rural Statistics Yearbook. Guangdong Rural Statistics Yearbook 2000 [M]. Beijing: China Statistics Press, 2001.
[49] Editorial Committee of the Guangdong Rural Statistics Yearbook. Guangdong Rural Statistics Yearbook 2010 [M]. Beijing: China Statistics Press, 2011.
[50] Editorial Committee of the Guangdong Rural Statistics Yearbook. Guangdong Rural Statistics Yearbook 2019 [M]. Beijing: China Statistics Press, 2020.
[51] Energy Division, National Statistical Office. China Energy Statistics Yearbook 1990 [M]. Beijing: China Statistics Press, 1991.
[52] Energy Division, National Statistical Office. China Energy Statistics Yearbook 2000 [M]. Beijing: China Statistics Press, 2001.
[53] Energy Division, National Statistical Office. China Energy Statistics Yearbook 2010 [M]. Beijing: China Statistics Press, 2011.
[54] Energy Division, National Statistical Office. China Energy Statistics Yearbook 2019 [M]. Beijing: China Statistics Press, 2020.
[55] China Communications and Transportation Association. Yearbook of China Intergrated transport 1990 [M]. Beijing: China Communications and Transportation Association, 1991.
[56] China Communications and Transportation Association. Yearbook of China Intergrated transport 2000 [M]. Beijing: China Communications and Transportation Association, 2001.
[57] China Communications and Transportation Association. Yearbook of China Intergrated transport 2010 [M]. Beijing: China Communications and Transportation Association, 2011.
[58] China Communications and Transportation Association. Yearbook of China Intergrated transport 2019 [M]. Beijing: China Communications and Transportation Association, 2020.
[59] Ministry of Agriculture and Rural Affairs, Bureau of Fisheries and Fishery Administration, National General Station for the Promotion of Aquatic Technology, Chinese Society of Fisheries. China Fishery Statistical Yearbook 1990 [M]. Beijing: China Agriculture Press, 1991.
[60] Ministry of Agriculture and Rural Affairs, Bureau of Fisheries and Fishery Administration, National General Station for the Promotion of Aquatic Technology, Chinese Society of Fisheries. China Fishery Statistical Yearbook 2000 [M]. Beijing: China Agriculture Press, 2001.
[61] Ministry of Agriculture and Rural Affairs, Bureau of Fisheries and Fishery Administration, National General Station for the Promotion of Aquatic Technology, Chinese Society of Fisheries. China Fishery Statistical Yearbook 2010 [M]. Beijing: China Agriculture Press, 2011.
[62] Ministry of Agriculture and Rural Affairs, Bureau of Fisheries and Fishery Administration, National

General Station for the Promotion of Aquatic Technology, Chinese Society of Fisheries. China Fishery Statistical Yearbook 2019 [M]. Beijing: China Agriculture Press, 2020.
[63] Department of Marine Strategic Planning and Economics, Ministry of Natural Resources, P. R. China. China Marine Economic Statistical Yearbook 1992 [M]. Beijing: China Ocean Press, 1993.
[64] Department of Marine Strategic Planning and Economics, Ministry of Natural Resources, P. R. China. China Marine Economic Statistical Yearbook 2000 [M]. Beijing: China Ocean Press, 2001.
[65] Department of Marine Strategic Planning and Economics, Ministry of Natural Resources, P. R. China. China Marine Economic Statistical Yearbook 2010 [M]. Beijing: China Ocean Press, 2011.
[66] Department of Marine Strategic Planning and Economics, Ministry of Natural Resources, P. R. China. China Marine Economic Statistical Yearbook 2019 [M]. Beijing: China Ocean Press, 2020.
[67] China Automotive Technology Research Center. China Automotive Industry Yearbook 1990 [M]. Tianjin: China Association of Automobile Manufacturers (CAAM), 1991.
[68] China Automotive Technology Research Center. China Automotive Industry Yearbook 2000 [M]. Tianjin: China Association of Automobile Manufacturers (CAAM), 2001.
[69] China Automotive Technology Research Center. China Automotive Industry Yearbook 2010 [M]. Tianjin: China Association of Automobile Manufacturers (CAAM), 2011.
[70] China Automotive Technology Research Center. China Automotive Industry Yearbook 2019 [M]. Tianjin: China Association of Automobile Manufacturers (CAAM), 2020.
[71] China Electricity Council. China Electricity Statistical Yearbook 1992 [M]. Beijing: China Electric Power Press, 1993.
[72] China Electricity Council. China Electricity Statistical Yearbook 2000 [M]. Beijing: China Electric Power Press, 2001.
[73] China Electricity Council. China Electricity Statistical Yearbook 2010 [M]. Beijing: China Electric Power Press, 2011.
[74] China Electricity Council. China Electricity Statistical Yearbook 2019 [M]. Beijing: China Electric Power Press, 2020.
[75] Urban Socio-Economic Surveys Division, National Bureau of Statistics. China City Statistical Yearbook 1990 [M]. Beijing: China Statistics Press, 1991.
[76] Urban Socio-Economic Surveys Division, National Bureau of Statistics. China City Statistical Yearbook 2000 [M]. Beijing: China Statistics Press, 2001.
[77] Urban Socio-Economic Surveys Division, National Bureau of Statistics. China City Statistical Yearbook 2010 [M]. Beijing: China Statistics Press, 2011.
[78] Urban Socio-Economic Surveys Division, National Bureau of Statistics. China City Statistical Yearbook 2019 [M]. Beijing: China Statistics Press, 2020.
[79] Tang, Y. Z., Wang, M. D., Liu, Q., *et al*. Ecological carrying capacity and sustainability assessment for coastal zones: A novel framework based on spatial scene and three-dimensional ecological footprint model [J]. *Ecological Modelling*, 2022, 466: 109881.
[80] Canton, H. Food and Agriculture Organization of the United Nations—FAO [M]//The Europa directory of international organizations 2021. Routledge, 2021: 297–305.
[81] Running, S., Zhao, M. MOD17A3HGF MODIS/terra net primary production gap-filled yearly L4 global 500 m SIN grid V006 [DB]. 2021. https://doi.org/10.5067/MODIS/MOD17A3HGF.006.
[82] Behrenfeld, M. J., Falkowski, P. G. Photosynthetic rates derived from satellite-based chlorophyll concentration [J]. *Limnology and Oceanography*, 1997, 42(1): 1–20.
[83] Liu, Y. M., Wang, Z. H., Yang, X. M., *et al*. Satellite-based monitoring and statistics for raft and cage aquaculture in China's offshore waters [J]. *International Journal of Applied Earth Observation and Geoinformation*, 2020, 91: 102118.
[84] Hu, Z. W., Li, Q. Q., Zou, Q., *et al*. A bilevel scale-sets model for hierarchical representation of large remote sensing images [J]. *IEEE Transactions on Geoscience and Remote Sensing*, 2016, 54(12): 7366–7377.
[85] Hu, Z. W., Wu, Z. C., Zhang, Q., *et al*. A spatially-constrained color-texture model for hierarchical VHR image segmentation [J]. IEEE Geoscience and Remote Sensing Letters, 2013, 10(1): 120–124.
[86] Liu, M. C., Li, W. H., Xie, G. D. Estimation of China ecological footprint production coefficient based on net primary productivity.[J]. *Chinese Journal of Ecology*, 2010, 29(3): 592–597.
[87] Fang, K. Ecological footprint depth and size: new indicators for a 3D model [J]. *Acta Ecologica Sinica*, 2013, 33(1): 267–274.
[88] Niccolucci, V., Galli, A., Reed, A., *et al*. Towards a 3D national ecological footprint geography [J]. *Ecological Modelling*, 2011, 222(16): 2939–2944.